A study of planar anchor groups for graphene-based single-molecule electronics

Steven Bailey, David Visontai, Colin J. Lambert, Martin R. Bryce, Harry Frampton, and David Chappell

Citation: The Journal of Chemical Physics **140**, 054708 (2014); doi: 10.1063/1.4861941
View online: http://dx.doi.org/10.1063/1.4861941
View Table of Contents: http://scitation.aip.org/content/aip/journal/jcp/140/5?ver=pdfcov
Published by the AIP Publishing

A study of planar anchor groups for graphene-based single-molecule electronics

Steven Bailey,[1] David Visontai,[1] Colin J. Lambert,[1,a)] Martin R. Bryce,[2] Harry Frampton,[3] and David Chappell[3]
[1]*Department of Physics, Lancaster University, Lancaster LA1 4YB, United Kingdom*
[2]*Department of Chemistry, Durham University, Durham DH1 3LE, United Kingdom*
[3]*BP Exploration Operating Company Limited, Chertsey Road, Sunbury on Thames, Middlesex TW16 7BP, United Kingdom*

(Received 14 September 2013; accepted 30 December 2013; published online 5 February 2014)

To identify families of stable planar anchor groups for use in single molecule electronics, we report detailed results for the binding energies of two families of anthracene and pyrene derivatives adsorbed onto graphene. We find that all the selected derivatives functionalized with either electron donating or electron accepting substituents bind more strongly to graphene than the parent non-functionalized anthracene or pyrene. The binding energy is sensitive to the detailed atomic alignment of substituent groups over the graphene substrate leading to larger than expected binding energies for –OH and –CN derivatives. Furthermore, the ordering of the binding energies within the anthracene and pyrene series does not simply follow the electron affinities of the substituents. Energy barriers to rotation or displacement on the graphene surface are much lower than binding energies for adsorption and therefore at room temperature, although the molecules are bound to the graphene, they are almost free to move along the graphene surface. Binding energies can be increased by incorporating electrically inert side chains and are sensitive to the conformation of such chains. © *2014 AIP Publishing LLC*. [http://dx.doi.org/10.1063/1.4861941]

I. INTRODUCTION

Functionalization of graphene and carbon nanotubes (CNTs) offers a potential route to molecular-scale electronics[1] and by increasing their solubility in water or organic solvents, has potential applications in biochemistry and materials science.[2,3] Covalent bonding of substituents to graphene or CNTs is an approach that has been widely exploited. However, this can have the undesirable effect of altering the intrinsic electronic properties of the graphene or CNT by breaking their extended π conjugation. By contrast, supramolecular (non-covalent) functionalization via π–π stacking has only a minimal effect on their electronic properties.[4–7] In this context, a range of polycyclic aromatics have been studied experimentally, including anthracene,[8–11] phenanthrene,[12,13] pyrene,[4,5,14–20] tetracene,[13] pentacene,[13] and diazapentacene.[21] Recent *ab initio* calculations[22,23] have focussed on the adsorption of planar unsaturated aromatic molecules onto a range of small-diameter CNTs. The results are sensitive to the chirality of the CNTs and to the orientation of the adsorbed molecule. In this article we study the opposite limit of planar molecules adsorbed onto graphene, which can also be viewed as a large-diameter CNT, whose curvature is sufficiently large to allow its surface to be regarded as almost planar, at least on the length-scale of the adsorbed molecule. Results are presented for the binding energetics of anthracene and pyrene based families of molecules, which suggest that these are ideal candidates for anchoring functional molecules to graphene and CNT surfaces.

a)Electronic mail: c.lambert@lancaster.ac.uk

II. METHODS

Both π–π stacking and van der Waals interactions make major contributions to binding energies and therefore we include both effects by using the density functional theory (DFT) package SIESTA[24] (which compares well with other implementations of DFT[25–31]), and a recently developed van der Waals density functional (vdW-DF),[32–34] which uses the revPBE35 revised version of the Perdew, Burke, and Ernzerhof generalised-gradient approximation exchange-correlation functional.[35] The vdW-DF used in SIESTA is a universal non-local density functional applicable to arbitrary geometries[36] and has been benchmarked recently by Carter and Rohl.[37] To describe π–π interactions, we used extended double zeta polarized basis sets of pseudo atomic orbitals and when optimising geometries, the atomic forces were relaxed to less than 20 meV/Å. The size of the unit cell was chosen to be 18.7 Å in the x direction, 20.7 Å in the y direction, and was periodic in the x and y directions. In the z direction, the separation was 20.0 Å, which ensured that the next unit was placed sufficiently far away to avoid any orbital interactions. Basis set superposition errors (BSSE) were avoided by retaining "ghost states" as prescribed in the counterpoise method.[38,39] This means that when calculating total energies of bound and unbound systems, the basis set remained fixed.

III. RESULTS AND DISCUSSION

To benchmark our calculations, we first computed the average binding energy per carbon atom, E^B of an A-B stacked graphene bi-layer. We obtained a binding energy of

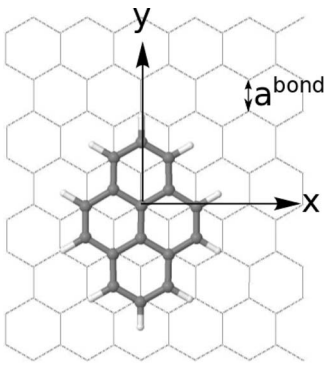

FIG. 1. Pyrene is A-B stacked at a separation $d = 3.44$ Å from the graphene sheet. The bond between two carbon atoms is $a^{bond} = 1.44$ Å for the vdW-DF.

$E^B = -48$ meV/C, which compares well with experimental results[40,41] which range from -30 to -50 meV/C. The average separation of the sheets was found to be 3.45 Å. For the case of a graphene tri-layer we find that the binding energy per carbon atom increases by 6% to $E^B = 51$ meV/C. The addition of further layers does not change E^B significantly.

Calculations to establish the position and orientation of the two families of adsorbed anthracene and pyrene derivatives on a graphene sheet also reveal that A-B stacking of the carbon atoms (see Figure 1) is the most favourable configuration. Table I shows changes in the binding energy (ΔE^B) when pyrene, 1-pyrenecarboxaldehyde, and 10-anthracenemethanol are rotated or displaced relative to the A-B stacked configuration. To calculate the energy barriers to rotation in the x-y plane we computed the changes in binding energy due to rotations of 10° and 20° about the atom at $x = y = 0$ and separately the energy changes due to displacements of $\frac{\sqrt{3}}{4}a^{bond}$ in the x direction and of $\frac{1}{2}a^{bond}$ in the y direction. Table I shows the results for ΔE^B due to these deviations from the A-B stacked configuration and demonstrates that A-B stacking is the most energetically favourable geometry. The energy barriers due to a displacement from A-B stacking are comparable with k_BT at room temperature (0.025 eV) and therefore at this temperature, the molecules will be mobile over the graphene surface.

As a further benchmark of our methodology, for benzene, naphthalene, anthracene, and pyrene, Figure 3(a) shows a plot of the binding energies per carbon atom versus N_H/N_C, where

TABLE I. This table shows ΔE^B (eV) for the three molecules due to rotations of 10° and 20° or displacements parallel to the graphene surface of $\frac{\sqrt{3}}{4}a^{bond}$ in the x direction and of $\frac{1}{2}a^{bond}$ in the y direction, where $a^{bond} = 1.44$ Å.

Derivative with rotation	ΔE^B (10°)	ΔE^B (20°)
Pyrene	+0.01	+0.02
1-pyrenecarboxaldehyde	+0.02	+0.02
10-anthracenemethanol	+0.02	+0.02
Derivative with shift	ΔE^B in x	ΔE^B in y
Pyrene	+0.01	+0.01
1-pyrenecarboxaldehyde	+0.02	+0.02
10-anthracenemethanol	+0.02	+0.02

TABLE II. This table shows the binding energies (E^B (eV)) to graphene of anthracene derivatives and their separation d (Å) from the graphene sheet. The coverage results are found in Ref. 8.

Molecule on a graphene sheet	E^B (eV)	d (Å)	Coverage[a]
Anthracene	−1.03	3.45	2%
Anthracene on bi-layer graphene	−1.06	3.45	
10[b]-anthracenemethanol	−1.20	3.44	6%
1,2,10-anthracenetriol	−1.21	3.44	0.03%
9,10-anthracenedicarbonitrile	−1.23	3.44	6%
1,2-dihydroxyanthracene	−1.16	3.44	
Decahydroxyanthracene	−1.61	3.44	
9,10-difluoroanthracene	−1.15	3.44	
9,10-dichloroanthracene	−1.14	3.45	
9,10-dibromoanthracene	−1.12	3.50	5%
9,10-diiodoanthracene	−1.07	3.55	
decafluoroanthracene	−1.35	3.44	

[a]Data for coverage on the sidewalls of SWNTs reported in Ref. 8.
[b]Refers to the numbering system as shown for 1,2,10-anthracenetriol in Figure2.

N_C is the number of carbon atoms and N_H is the number of hydrogen atoms per molecule. The black line shows the interpolation formula[42] $E^B = N_C E_{CC} + N_H(E_{CH} - E_{CC})$, with $E_{CC} = -49.2$ meV/C and $E_{CH} = -80.1$ meV/H. In agreement with Ref. 42 we find that A-B stacking is the most favourable. In our simulations, the molecules and graphene are allowed to distort, whereas in Ref. 42 the molecules and graphene are constrained to remain planar. This distortion is particularly evident for naphthalene and anthracene, which accounts for their deviation from the straight line.

The main results of our calculations of binding energies for anthracene and pyrene derivatives on a graphene sheet are presented in Tables II and IV. To clarify the position of functional groups of the anthracene derivatives relative to the graphene sheet, we have assigned an index n to each carbon atom as shown in Figure 2.

In Table II the results show E^B for a number of anthracene derivatives, five of which were studied experimentally by Zhang *et al.*,[8] who measured the maximum coverage of each molecule on single-walled carbon nanotubes (SWNTs). These

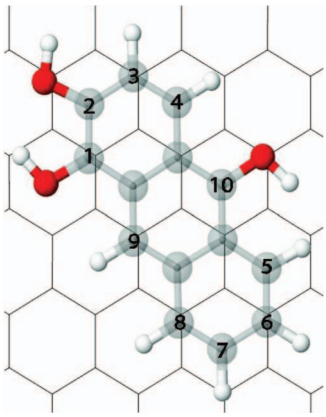

FIG. 2. The image for 1,2,10-anthracenetriol absorbed onto a graphene sheet illustrates the A-B stacked configuration which, as for pyrene, is most energetically favorable for these anthracene derivatives. The carbon sites available for functionalisation are numbered by an index n from 1 to 10.

TABLE III. The van der Waals radii (R^{vdW} (Å)) of the elements used in this study.

Element	H	F	O	N	C	Cl	S	Br	I
R^{vdW} (Å)	1.09	1.47	1.52	1.55	1.70	1.75	1.80	1.85	1.98

measured coverages are shown in the right-most column of the table.

If the experimental coverage for 1,2,10-anthracenetriol is ignored, then the two highest measured coverages (9,10-anthracenedicarbonitrile and 10-anthracenemethanol) correspond to the two highest binding energies, predicted in the present work; the lowest coverage (anthracene) corresponds to the lowest predicted binding energy; and the intermediate coverage (9,10-dibromoanthracene) corresponds to the intermediate binding energy, as expected. Interestingly, this ordering does *not* follow the order of the electron affinities for these molecules, since the electron affinity of 9,10-dibromoanthracene is higher than that of 10-anthracenemethanol, due to the presence of the electron-withdrawing bromine substituents. By contrast, the binding energies calculated for the 9,10-dihalo anthracene derivatives, shown in Table II, increase with the order of the predicted electronegativity for each halogen and the associated decrease in the vdW radii (see Table III). The conformations of these molecules adsorbed onto a graphene sheet are shown in Figure 2 of the supplementary material.[43]

Clearly the measured coverage of 1,2,10-anthracenetriol does not correlate with its high binding energy. To demonstrate that the high binding energy of 1,2,10-anthracenetriol is nevertheless reasonable, Figure 3(b) shows the change in the binding energy when the number of m of –OH groups is increased. Clearly 1,2,10-anthracenetriol sits on the trend line, which takes the form $E^B = (\Delta E^B)m + E_0$, where $\Delta E^B) = -57.2$ meV and $E_0 = -1.037$ eV. A more detailed inspection of the change in binding energy with the number of −OH groups reveals that the change depends on the precise location of the −OH group. As shown in Figure 2, anthracene possesses 10 possible attachment sites. For $n = 2$, 4, 5, 7, and 10, the hydrogen in the −OH group sits above the centre of a hexagon of the graphene sheet and therefore we denote this position H^{hex}. For $n = 1$, 3, 6, 8, and 9, the hydrogen on the −OH group sits over a carbon atom of the graphene and we denote this position H^{carbon}. Figure 3(c) shows the change in binding energy ΔE_n^B which occurs when a single −OH group is attached to different sites labelled n of the anthracene molecule. This shows that the extra binding energy due to H^{carbon} −OH groups is −64 meV, whereas the extra binding energy due to H^{hex} −OH groups varies between −45 and −54 meV. These differences are reflected in their distances from the graphene, dz which is defined as the perpendicular distance of the hydrogen on the −OH group from the graphene surface. These are >3.0 Å for H^{hex} and <3.0 Å for H^{carbon}.

Table II shows that compared with the non-functionalised aromatic skeleton, the binding energy is increased by the presence of either electron-donating or electron-accepting

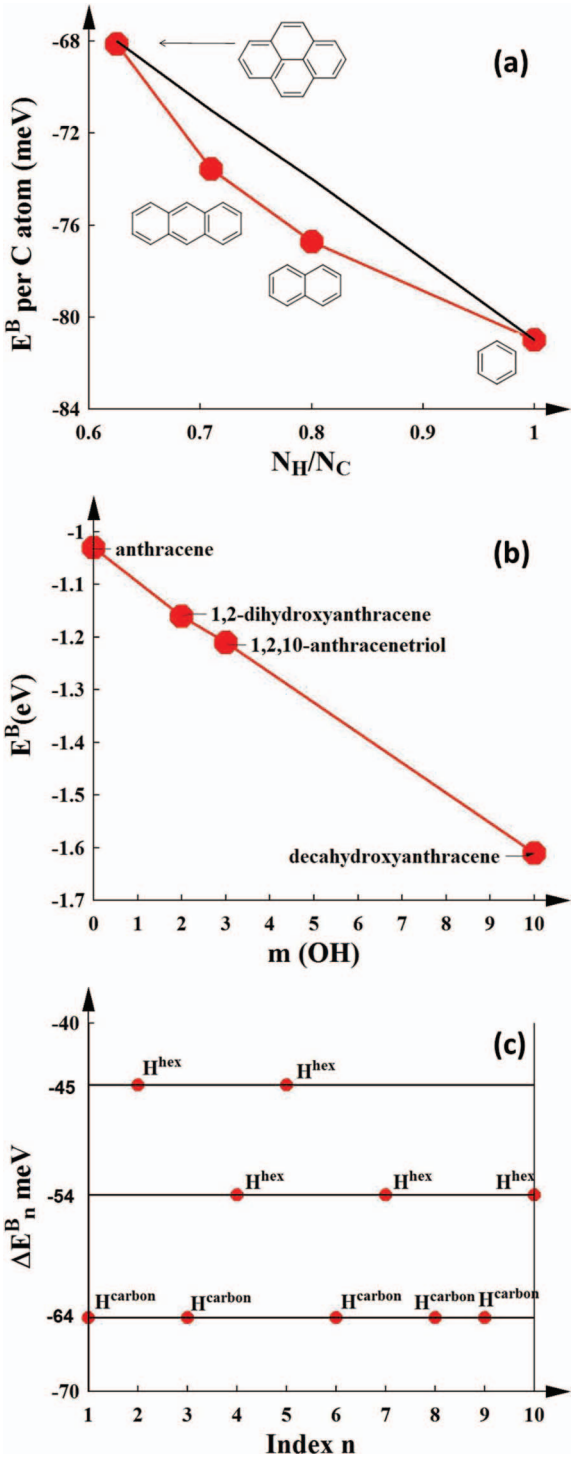

FIG. 3. (a) The binding energy per carbon atoms as a function of N_H/N_C, where N_C is the number of carbon atoms and N_H is the number of hydrogen atoms per molecule. (b) The variation in binding energy of anthracene derivatives versus the number m of OH groups. (c) The change in binding energy when a single OH group is added to different locations of the parent anthracenes, indicated by an index n (see Fig. 2).

substituents. To understand this behaviour, we first compare the two extremes of anthracene (donor) and decafluoroanthracene (acceptor). In anthracene, the hydrogen atoms all donate fractions of an electron directly onto the ten outer carbon atoms, which in the nomenclature of Hunter and Sanders[44] are, therefore, π rich (i.e., negatively charged). Five of these

ten atoms (H^{carbon} indexed $n = 1, 3, 6, 8, 9$ in Figure 2) are π–π stacked directly above carbon atoms of the graphene substrate. Therefore, these atoms contribute to inter-layer *repulsion*. In the case of decafluoroanthracene, the polarity of these sites is reversed, resulting in these sites contributing to inter-layer *attraction*. We find that all the substituents (whether electron donating or accepting) reduce the net negative charge or even reverse the sign of the net charge transferred onto the anthracene skeleton at the points of attachment (compared to unsubstituted anthracene). Therefore, all the substituents in Table II decrease the π–π repulsion at these sites. Consequently, the overall result is always an increase in the binding energy.

In the case of the H^{carbon} configurations these carbons possess an opposite sign to the hydrogen atoms and consequently, in addition to a reduction in π–π repulsion, there is an additional attraction, which is highly dependent upon the separation dz. This additional attraction is also present in the H^{hex} configurations and is also seen to depend upon the separation dz.

As in the above result for a graphene tri-layer the binding energy of anthracene increases from −1.03 eV when adsorbed onto a graphene mono-layer to −1.06 eV on a graphene bi-layer, which is a 3.2% increase.

For the molecules reported in Ref. 8, Table II shows that 9,10-anthracenedicarbonitrile has the highest binding energy of $E^B = -1.23$ eV. This illustrates the importance of the detailed atomic alignment of the substituent over the graphene sheet. The nitrogen in the −CN group lies over a carbon atom at a separation of 3.37 Å (compared to 3.50 Å for one of the central anthracene carbons).

In Ref. 8, Zhang *et al.* reported an anomalously low coverage (0.03%) for 1,2,10-anthracenetriol on SWNTs based on the experimentally measured fluorescence intensity of the adsorptive adduct relative to free 1,2,10-anthracenetriol. The coverage of other derivatives in that study was estimated based on UV-vis absorption spectra; no bands in the absorption spectra could be detected for the adsorption of 1,2,10-anthracenetriol. However, the authors do not discuss the possibility that if 1,2,10-anthracenetriol is strongly bound to the SWNTs (as may be the case based on our calculations on graphene in Table II) quenching of the fluorescence would be expected due to an electronic interaction in the excited state, which would give an apparent low coverage on the SWNTs. Fluorescence quenching studies of SWNT-anthracene adducts have been reported.[9–11]

In Table IV the binding energies of a number of pyrene derivatives are presented. As expected, due to the larger footprint of pyrene the binding energy E^B is higher than for that of anthracene. Nevertheless, it is interesting to note that some anthracene derivatives have a higher binding energy than non-functionalised pyrene and should therefore will have a tendency to displace it from a graphene surface. In addition to −OH groups, longer-chain substituents can also lead to high binding energies. This is illustrated by comparing the high binding energy (−1.54 eV) of 1-pyrenebutyric acid calculated when the butyric acid side group is bound to the graphene sheet, with the binding energy (−1.30 eV) of an alternative conformer in which the butyric acid chain is directed away from the graphene surface. This example demonstrates that the interaction of side chains with the surface can significantly increase the binding energy. Finally, we note that the high binding energy of 1,6-dithiapyrene is a special case. In this strong electron donor[45] two C-H units in the pyrene ring are substituted by sulfur atoms and the A-B geometry is replaced by an off-set arrangement, which favours a π–σ attractive interaction.[44] Following the previous argument this should produce a large binding energy but the larger vdW radius of the sulfur atoms interacts strongly with the graphene sheet which causes the sheet to warp and the sulfur atoms to be deflected away from the surface twisting the pyrene skeleton and pushing the derivative away from the surface. This has the effect of reducing the binding energy to a relatively low value of −1.14 eV as the average distance from the graphene plane increases to 3.55 Å.

TABLE IV. This table shows the binding energies E^B (eV) to graphene of pyrene derivatives and their separation d (Å) from the graphene sheet.

Molecule on a graphene sheet	E^B (eV)	d (Å)
Pyrene	−1.09	3.45
Pyrene on a graphene bi-layer	−1.12	3.45
1-pyrenecarboxaldehyde	−1.22	3.44
2-pyrenecarboxaldehyde	−1.23	3.44
1-chloropyrene	−1.15	3.45
1-aminopyrene	−1.19	3.44
1,6-dithiapyrene	−1.14	3.55
1-pyrenebutyric acid	−1.54	3.48
1-pyrenebutyric acid conformer	−1.30	3.49
1-methylpyrene	−1.20	3.44
2-pyreneacetaldehyde	−1.23	3.50
1-pyrenemethanol	−1.25	3.45
1-pyrenecarboxylic acid	−1.35	3.50
1-pyrenebutanol	−1.24	3.44

Our results have implications for calculations of electron transport through single molecules attached to carbon-based electrodes by planar anchor groups, as in Refs. 46 and 47. In particular, we have compared our results with the less-accurate local density approximation (LDA) and find that inclusion of vdW interactions significantly increase both the binding energy and inter-layer separation compared with bare LDA. Consequently the π–π electronic coupling between planar aromatics and graphene is weaker than that predicted by LDA (Ref. 48). This means that the latter will typically overestimate the electrical conductance of single molecules bound to CNT or graphene electrodes by planar aromatic anchors. vdW interactions also have a significant effect on the geometry of the system, because the interaction between the graphene and atoms with a large vdW radius (see Table III) causes the sheet to warp and also deflects the atoms away from the surface. This breaks the π–π conjugation by distorting the anthracene or pyrene skeleton and increases the average separation. Binding energies are also sensitive to the conformation of longer side groups relative to the graphene surface and can be significantly enhanced when such groups lie parallel to the surface. This is potentially useful for the design of single-molecule electronic devices, where electrically

inert side groups are often added to functional backbones to increase solubility.

IV. CONCLUSION

We have presented a systematic analysis of the binding energetics of anthracene- and pyrene-based families of molecules adsorbed onto graphene. DFT calculations show that for all derivatives studied, the binding energy is increased by the presence of either electron donating or electron accepting substituents. In most cases the functionalization of anthracene increases the binding energy of the derivative to a value greater than that of unsubstituted pyrene and therefore, the anthracene derivatives could displace pyrene from a graphene surface.

The –CN and –OH groups are the most effective substituents for enhancing binding to graphene, due to secondary attractive interactions with the graphene. Having identified the –OH group as a special case, we note that if the results in Ref. 8 for the derivatives with –OH groups are ignored, then the experimental adsorption coverages (i.e., 9,10-anthracenedicarbonitrile > 9,10-dibromoanthracene > anthracene) follow the same order as both the electron affinities and our computed binding energies (i.e., 9,10-anthracenedicarbonitrile > 9,10-dibromoanthracene > anthracene).

ACKNOWLEDGMENTS

We thank BP Exploration Operating Company Ltd. and the European Commission (EC) FP7 ITN "MOLESCO" Project No. 606728 for funding this work.

[1]P. Singh, S. Campidelli, S. Giordano, D. Bonifazi, A. Bianco, and M. Prato, Chem. Soc. Rev. **38**, 2214 (2009).
[2]E. A. Mayer, R. K. Castellano, and F. Diederich, Angew. Chem. Int. Ed. **42**, 1210 (2003).
[3]C. Backes and A. Hirsch, *Chemistry of Nanocarbons*, edited by T. Akasaka, F. Wudl and S. Nagase (Wiley, 2010), p. 1.
[4]Y. Zhang, C. Liu, W. Shi, Z. Wang, L. Dai, and X. Zhang, Langmuir **23**, 7911 (2007).
[5]J. Liu, O. Bibari, P. Mailley, J. Dijon, E. Rouviere, F. Sauter-Starace, P. Caillat, F. Vinet, and G. Marchand, New J. Chem. **33**(5), 1017 (2009).
[6]S. Grimme, Angew. Chem. Int. Ed. **47**, 3430 (2008).
[7]F. Tournus, S. Latil, M. I. Heggie, and J. C. Charlier, Phys. Rev. B **72**, 075431 (2005).
[8]J. Zhang, J. K. Lee, Y. Wu, and R. W. Murray, Nano Lett. **3**, 403 (2003).
[9]A. S. D. Sandanayaka, Y. Takaguci, T. Uchida, Y. Sako, Y. Morimoto, Y. Araki, and O. Ito, Chem. Lett. **35**, 1188 (2006).
[10]T. G. Hedderman, S. M. Keogh, G. Chambers, and H. J. Byrne, J. Phys. Chem. B **108**, 18860 (2004).
[11]T. G. Hedderman, S. M. Keogh, G. Chambers, and H. J. Byrne, J. Phys. Chem. B **110**, 3895 (2006).
[12]Y. Tomonari, H. Murakami, and N. Nakashima, Chem. Eur. J. **12**, 4027 (2006).
[13]S. Gotovac, H. Honda, Y. Hattori, K. Takahashi, H. Kanoh, and K. Kaneko, Nano Lett. **7**, 583 (2007).
[14]H. J. Chen, R. J. Zhang, Y. G. Wang, and D. W. Dai, J. Am. Chem. Soc. **123**, 3838 (2001).
[15]S. Y. Fernando, K. A. S. Lin, Y. Wang, W. Kumar, S. Zhou, B. Xie, Y. P. Cureton, and L. T. Sun, J. Am. Chem. Soc. **126**, 10234 (2004).
[16]C. Ehli, G. M. A. Rahman, N. Jux, D. Balbinot, D. M. Guldi, F. Paolucci, M. Marcaccio, D. Paolucci, M. Melle-Franco, F. Zerbettol, S. Campidelli, and M. Prato, J. Am. Chem. Soc. **128**, 11222 (2006).
[17]D. M. Guldi, G. M. Rashman, N. Jux, D. Balbinot, N. Tagmatarchis, and M. Prato, Chem. Commun. **15**, 2038 (2005).
[18]J. Bartelmess, B. Ballesteros, G. de la Torre, D. Kiessling, S. Campidelli, M. Prato, T. Torres, and D. M. Guldi, J. Am. Chem. Soc. **132**, 16202 (2010).
[19]T. J. Simmons, J. Bult, D. P. Hashim, R. J. Linhardt, and P. M. Ajayan, ACS Nano **3**, 865 (2009).
[20]C. L. Chung, C. Gautier, S. Campidelli, and A. Filoramo, Chem. Commun. **46**, 6539 (2010).
[21]A. Mateo-Alonso, C. Ehli, K. H. Chen, D. M. Guldi, and M. Prato, J. Phys. Chem. A **111**, 12669 (2007).
[22]N. Lim and S. Park, Appl. Phys. Lett. **95**, 243110 (2009).
[23]J. P. McNamara, R. Sharma, M. A. Vincent, I. H. Hillier, and C. A. Morgado, Phys. Chem. Chem. Phys. **10**, 128 (2008).
[24]J. M. Soler, E. Artacho, J. Gale, A. García, J. Junquera, P. Ordejón, and D. Sánchez-Portal, J. Phys. Condens. Matter **14**, 2745 (2002).
[25]S. Barraza-Lopez, K. Park, V. García-Suarez, and J. Ferrer, Phys. Rev. Lett. **102**, 246801 (2009).
[26]S. Barraza-Lopez, K. Park, V. García-Suarez, and J. Ferrer, J. Appl. Phys. **105**, 07E309 (2009).
[27]D. C. Langreth, B. I. Lundqvist, S. D. Chakarova-Kack, V. R. Cooper, M. Dion, P. Hyldgaard, A. Kelkkanen, J. Kleis, L. Kong, S. Li, P. G. Moses, E. Murray, A. Puzder, H. Rydberg, E. Schroder, and T. Thonhauser, J. Phys. Condens. Matter **21**, 084203 (2009).
[28]K. Lee, E. D. Murray, L. Kong, B. I. Lundqvist, and D. C. Langreth, Phys. Rev. B **82**, 081101 (2010).
[29]S. D. Chakarova-Käck, E. Schröder, B. I. Lundqvist, and D. C. Langreth, Phys. Rev. Lett. **96**, 146107 (2006).
[30]S. D. Chakarova-Käck, O. Borck, E. Schröder, and B. I. Lundqvist, Phys. Rev. B **74**, 155402 (2006).
[31]K. Berland, S. Chakarova-Kack, V. R. Cooper, D. C. Langreth, and E. Shroder, J. Phys. Condens. Matter **23**, 135001 (2011).
[32]M. Dion, H. Rydberg, E. Schröder, D. C. Langreth, and B. I. Lundqvist, Phys. Rev. Lett. **92**, 246401 (2004).
[33]D. C. Langreth, M. Dion, H. Rydberg, E. Schröder, P. Hyldgaard, and B. I. Lundqvist, J. Quantum Chem. **101**, 599 (2005).
[34]M. Dion, H. Rydberg, E. Schröder, D. C. Langreth, and B. I. Lundqvist, Phys. Rev. Lett. **95**, 109902(E) (2005).
[35]Y. Zhang and W. Yang, Phys. Rev. Lett. **80**, 890 (1998).
[36]J. M. Román-Pérez and J. M. Soler, Phys. Rev. Lett. **103**, 096102 (2009).
[37]D. J. Carter and A. L. Rohl, J. Chem. Theory Comput. **8**, 281 (2012).
[38]P. Jansen, H. B. Ross, and J. M. Soler, Chem. Phys. Lett. **3**, 140 (1969).
[39]F. Boys and S. F. Bernardi, Mol. Phys. **19**, 553 (1970).
[40]V. H. Benedict, L. X. Chopra, N. G. Cohen, M. L. Zettl, A. Louie, and S. G. Crespi, Chem. Phys. Lett. **286**, 490 (1998).
[41]T. Zacharia, R. Ulbricht, and H. Hertel, Phys. Rev. B **69**, 155406 (2004).
[42]J. Björk, F. Hanke, C.-A. Palma, P. Samori, M. Cecchini, and M. Persson, J. Phys. Chem. Lett. **1**, 3407 (2010).
[43]See supplementary material at http://dx.doi.org/10.1063/1.4861941 for conformations of molecules analysed in this manuscript.
[44]J. K. M. Hunter and C. A. Sanders, J. Am. Chem. Soc. **112**, 5525 (1990).
[45]D. M. Guldi, F. Spänig, D. Kreher, I. F. Perepichka, C. van der Pol, M. R. Bryce, K. Ohkubo, and S. Fukuzumi, Chem. Eur. J. **14**, 250 (2008).
[46]C. W. Marquardt, S. Grunder, A. Blaszczyk, S. Dehm, F. Hennrich, H. V. Löhneysen, M. Mayor, and R. Krupke, Nature Nano. **5**, 863 (2010).
[47]F. Prins, A. Barreiro, J. W. Ruitenberg, J. S. Seldenthuis, N. Aliaga-Alcalde, L. M. K. Vandersypen, and H. S. J. van der Zant, Nano Lett. **11**, 4607 (2011).
[48]C. G. Péterfalvi and C. J. Lambert, Phys. Rev. B **86**, 085443 (2012).